

---

This is an electronic reprint of the original article.  
This reprint may differ from the original in pagination and typographic detail.

Keitaanniemi, Aino; Kukko, Antero; Virtanen, Juho-Pekka; Vaaja, Matti Tapio  
**Measurement Strategies for Street-Level SLAM Laser Scanning of Urban Environments**

*Published in:*  
Photogrammetric Journal of Finland

*DOI:*  
[10.17690/020271.1](https://doi.org/10.17690/020271.1)

Published: 01/01/2020

*Document Version*  
Publisher's PDF, also known as Version of record

*Please cite the original version:*  
Keitaanniemi, A., Kukko, A., Virtanen, J.-P., & Vaaja, M. T. (2020). Measurement Strategies for Street-Level SLAM Laser Scanning of Urban Environments. *Photogrammetric Journal of Finland*, 27(1), 1-19.  
<https://doi.org/10.17690/020271.1>

---

This material is protected by copyright and other intellectual property rights, and duplication or sale of all or part of any of the repository collections is not permitted, except that material may be duplicated by you for your research use or educational purposes in electronic or print form. You must obtain permission for any other use. Electronic or print copies may not be offered, whether for sale or otherwise to anyone who is not an authorised user.

## MEASUREMENT STRATEGIES FOR STREET-LEVEL SLAM LASER SCANNING OF URBAN ENVIRONMENTS

Aino Keitaanniemi <sup>1\*</sup>, Antero Kukko <sup>1,2</sup>, Juho-Pekka Virtanen <sup>1,2</sup> and Matti T. Vaaja <sup>1</sup>

<sup>1</sup> Department of Built Environment, School of Engineering, Aalto University, P.O. Box 14100, FI-00076 Aalto, Finland

<sup>2</sup> Finnish Geospatial Research Institute FGI, Geodeetinrinne 2, FI-02430 Masala, Finland

aino.keitaanniemi@aalto.fi, antero.kukko@nls.fi, juho-pekka.virtanen@aalto.fi,  
matti.t.vaaja@aalto.fi

### ABSTRACT

*Data collection for street-level mapping is currently executed with terrestrial (TLS) or mobile laser scanners (MLS). However, these methods have disadvantages such as TLS requiring a lot of time and MLS being dependent on the global navigation satellite system (GNSS) and an inertial measurement unit (IMU). These are not problems if we use simultaneous localization and mapping (SLAM) based laser scanners. We studied the utility of a SLAM ZEB-REVO scanner for mapping street-level objects in an urban environment by analyzing the geometric and visual differences with a TLS reference. In addition to this, we examined the influence of traffic on the measurement strategy. The results of the study showed that SLAM-based laser scanners can be used for street-level mapping. However, the measurement strategy affects the point clouds. The strategy of walking trajectory in loops produced a 2 cm RMS and 4-6 mm mode of error even in not optimal situations of the sensor in the urban environment. However, it was possible to get an RMS under 2.2 cm and a 32 cm mode of error with other measurement strategies.*

### 1. INTRODUCTION

The most of the current city models are produced from the aerial data (Valencia et al. 2015, Lee and Yang 2018, City of Helsinki 2019, GIM 2019, and Rotterdam 2019). However, the combination of aerial and ground-based data collection (hybrid) has become popular because of more accurate geometry of objects and texture quality (Lee and Yang 2018). One example of a hybrid city model is the city model of Zürich, which combines aerial and ground images (ETHZurich 2019). The next generation of hybrid city modeling could use ground-based measurement methods, such as mobile laser scanning systems or simultaneous localization and mapping (SLAM) based laser scanners, for mapping street-level object geometry (Haala et al. 2008, Zhu et al. 2011, Adán et al. 2019, and Ma et al. 2018). The ground-based measurements could cover boroughs of cities more accurately or even connect indoor spaces to the city model. With data from indoors the monitoring and planning of city areas would be more comprehensive.

SLAM-based laser scanners have many advantages versus stationary terrestrial laser scanners (TLS) and mobile laser scanners (MLS). TLS measurements take a relatively long time and MLS is dependent on direct georeferencing devices including the global navigation satellite system (GNSS) assisted with an inertial measurement unit (IMU). The most prominent advantages of SLAM-based systems are (1) more effective data collection than that of TLS because there is no need for multiple stationary measurement stations and their mutual registration, and (2) SLAM scanning can reach areas where GNSS positioning is not available, for example, in indoor and

underground environments (Adán et al. 2019, Ma et al. 2018, Sirmacek et al. 2016, and Holland et al. 2016). It has also been shown that SLAM-style algorithms can be applied to improve GNSS localization in challenging environments (Kukko et al. 2017). With these methods, city modeling could be facing a new era where data capture and subsequent modeling are carried out at street-level. In addition, this may be a key element in creating comprehensive 3D city models by only using point clouds as presented, e.g., by Nebiker et al. (2010) and Virtanen et al. (2017).

There are many SLAM-based laser scanners on the market, such as the Stencil and Contour from Kaarta, the Paracosm PX-80 and the Leica Pegasus Backpack. However, perhaps the most popular device has been the Zebedee by GeoSLAM. After GeoSLAM released the first ZEB1 model in 2013, there has been a great deal of research into how the Zebedee laser scanners perform and what applications they can be used for (Cadge 2016). Some of the applications include underground mines (Zlot & Bosse 2014, Dewez et al. 2016, Eyre et al. 2016, Dewez et al. 2017, and Frangez et al. 2018); indoor environments; as-built information modelling and indoor navigation models (Thomson et al. 2013, Sepasgozar et al. 2014, Sirmacekaet al. 2016, Manan Samad et al. 2016, Maboudi et al. 2017, Lehtola et al. 2017, Nocerino et al. 2017, Staats et al. 2017, and Chiabrando et al. 2018); cultural heritage sites (Zlot et al. 2014, Farella et al. 2016, Micoli et al. 2018, and Tucci et al. 2018); landform mapping and tree modelling (So et al. 2015, Vanneschi et al. 2017, and Cabo et al. 2018); and multi-sensor surveys (Sammartano & Spanò 2018). In all of these applications, testing the system performance outdoors has been only a minor topic.

The existing research on the outdoor use of SLAM systems can be categorized into three groups: (1) application tests; (2) filling of other point cloud data; and (3) experiments on how the SLAM system algorithm works in different situations. In (1), there have been several studies comparing Zebedee systems with other mobile laser scanners in outdoor applications. Tucci et al. (2018) and Nocerino et al. (2017) have tested the Zebedee on cultural heritage sites and Frangez et al. (2018) have performed experiments for gold mine modelling. In the research by Tucci et al. (2018), the ZEB-REVO was found to be the best of the laser scanners examined for measuring renaissance fortresses. However, it was found to face some problems in reconstructing planar and spherical targets and capturing small architectural details (Tucci et al. 2018). In Nocerino et al. (2017) the ZEB-REVO was also found to be the most suitable for measuring a cathedral square of the two systems investigated in the study. In the study, the researchers also observed some registration errors in the measurements (Nocerino et al. 2017). Frangez et al. (2018) noticed that the ZEB-REVO had some advantages for mine modelling over terrestrial laser scanners.

In the second category, the use of the Zebedee for filling unmanned aerial vehicle (UAV) or TLS data has been reported by Vanneschi et al. (2017) and So et al. (2015) in mining and risk management applications. In these studies, it was proven that the Zebedee system can fill UAV, MLS and aerial laser scanning (ALS) data at a reasonable level of spatial accuracy. Approaching the third category, So et al. (2015) also proved that the maximum practical measurement distance with the Zebedee system outdoors was 15 m. They also tested the ability of SLAM systems in several outdoor conditions, for example near a rocky stream, on a rock slope, at a landslide site and on a natural hillside. The results of these tests show that it is possible to successfully use the Zebedee system in those conditions. Outdoors the Zebedee system can detect the main elements of target objects. However, Zlot et al. (2014) noticed that the point density depends on the measurement speed and misalignment errors of tens of centimeters were found when the target object was far away. Additionally, results from data filling studies suggest better point cloud registration results when target objects were scanned in two passes and that the drift error of the measurements could be minimized with a well-planned trajectory (Sammartano & Spanò 2018, and

Chiabrando et al. 2018). This highlights the importance of measurement strategy, in practice path planning, when performing SLAM-based MLS surveys.

The objective of this study is to evaluate the impact of different measurement strategies on performance of SLAM laser scanning for mapping street-level urban environments. More precisely, the aim is to determine how different measurement strategies (path planning) affect street-level object mapping. We collected urban point cloud datasets using a ZEB-REVO handheld laser scanning system. The datasets included three alternative measurement trajectory strategies: (1) walking around buildings to form closed loops, (2) walking back and forth in front of buildings and (3) walking trajectory in loops. The differences of these measurement strategies help to plan and optimize SLAM-based laser scanning trajectory for mapping street-level urban environments. We look at the potential influence of different measurement strategies on the building facades, sidewalks and street objects by comparing the geometric and visual differences in the collected data against a reference dataset. Additionally, we discuss the influence of traffic on the measurement strategies. It was done by analyzing the number and type of vehicles visible in the data during the scans, and SLAM conditions (GeoSLAM 2017) between the measurement strategies.

## 2. MATERIALS AND METHODS

### 2.1 Study site

The experiments were performed on the Aalto University campus in Espoo, Finland, focusing on the vicinity of Vuorimiehentie Street. The more specific study site is illustrated in Figure 1. The buildings of the street are three and four floor office buildings. The street scene represents a typical urban environment with features, such as trees, bus stops and alley crossings between the buildings, which are common in almost any urban scene.

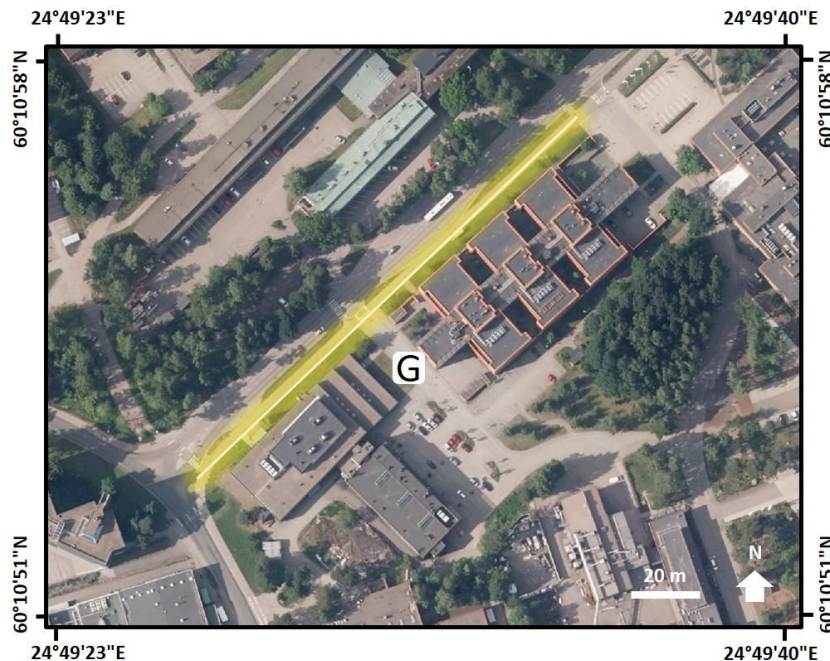


*Figure 1. An aerial photograph of the study area. The test site is marked in yellow, and is 210 m in length. The gap between the buildings is marked with letter G. (Ortophotograph © Espoo City Survey Department, 2017)*



Figure 2. The gap between the buildings is 22 m wide, with some road signs and a tree.

The study site has some features, which potentially make SLAM-based laser scanning complicated. The road next to the study area is busy with frequent bus, car and truck traffic. The width of the street is 21 m including the sidewalks. The gap between the two opposing buildings next to the roadside is 22 m (Figure 2). Given the ranging capability of the ZEB-REVO system (15-20 m (Cadge 2016)) the selected scene may assume geometric challenges for data acquisition and SLAM computation.

## 2.2 The reference data

The geometric reference data of the street was collected with a Faro Focus 3D 120S laser scanner, having a nominal range accuracy of  $\pm 2$  mm. To register the individual scans, we used six target spheres, which were 9 cm in radius. The target locations were changed by moving one or two of the target spheres at a time to follow the progress of the scanning. Altogether, there were 17 scanning stations and 21 target sphere locations, which are shown in Figure 3. The scan parameter settings for most of the TLS scans were 6 mm in resolution at a 10 m distance with noise reduction using three repeated laser measurements. Altogether there were 16 scans with 6 mm resolution, and a single scan between the buildings at resolution of 3 mm at a 10 m distance. The noise reduction remained the same for all of the scans. The registration of the 17 scans was accomplished using the Faro Scene software (version 6.0.2.23). The resulting point cloud registration had a 6.4 mm mean point error, a 18.0 mm maximum point error and a 56.8% minimum overlap.

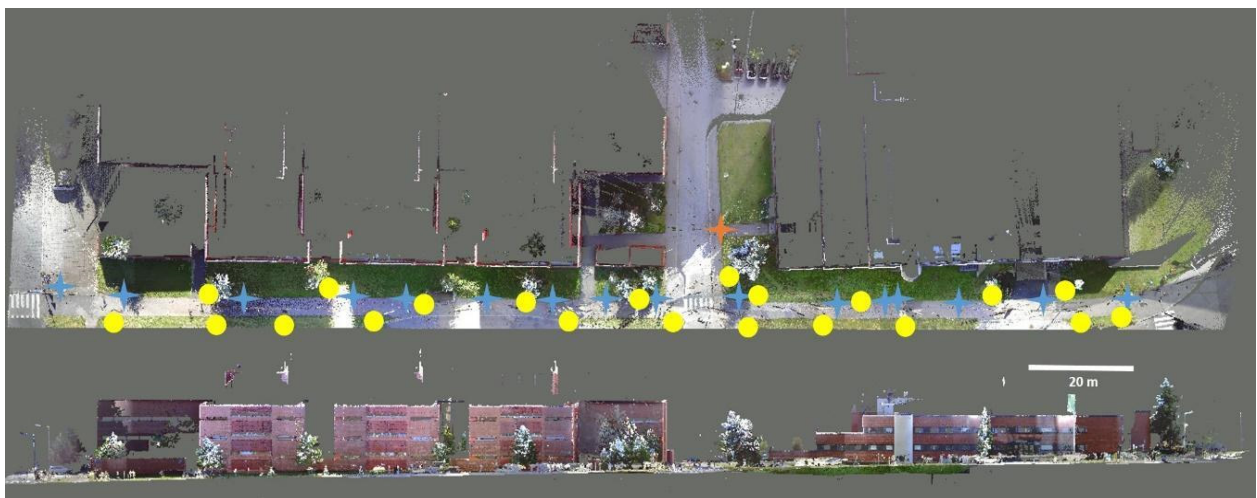


Figure 3. The reference point cloud from the top and a side view along the street. The scan locations are marked as blue stars except for the orange star, which was executed with different settings. The target sphere locations are shown as yellow dots.

### 2.3 The utilized SLAM system and measurement strategies

The SLAM laser scanner selected for the case study was the ZEB-REVO scanner, which GeoSLAM released in 2016. The ZEB-REVO system uses a Hokuyo UTM-30LX laser sensor, which rotates continuously around the front pointing axis (Bosse et al. 2012). The relative accuracy of the scanner is 1-3 cm and the maximum measurement distance is between 15 m outdoors and 30 m indoors. The rotation speed of the laser sensor is 0.5 Hz. The scanner profile frequency is 100 Hz and the data acquisition rate is 43,200 points/sec (Cadge 2016). The SLAM algorithm of the ZEB-REVO scanner uses surface elements, which are matched to the point cloud and IMU parameters to compute a map of the environment. The computation is an iterative process. First, the point cloud is split into smaller slices according to the acquisition time. From these slices, the algorithm recognizes planar surface elements. Then the algorithm matches the detected surface elements of the following slices with the knowledge of the IMU parameters and corrects the trajectory with the matching information (Bosse et al. 2012).

In our experiment with the ZEB-REVO, we utilized three different closed loop strategies, which are listed in Table 1. In the first strategy, we collected data by walking around buildings 1 and 3 anticlockwise, as shown in Figure 4. This was repeated three times in separate measurements. With this strategy, we investigated whether it was possible to speed up the data collection by passing the measurement area only once. In the second strategy, the data was collected by detecting objects twice during the measurement, but from different directions. This was implemented by walking back and forth along the street while trying to maintain the same distance to the buildings in both directions, as much as possible. We repeated the measurement with different traffic conditions, because this method results in the largest number of vehicles passing while measuring. This strategy tests whether there are advantages when the area of interest is measured twice during the scanning. In the third strategy, we carried out the measurement by walking trajectory in loops, which includes loops around objects to maximize overlap of scanning profiles around the objects as in the Figure 4d. The objects such as poles, trees and bus stop in the study site are visible in Figure 5. We walked back and forth along the street and around every tree (to cover the otherwise occluded building wall sections) on the street side. With this strategy we examined whether it would substantially improve the accuracy and whether it was a significantly slower data collection strategy than the other two. The approximate speed of the walking was 5 km/h for all the implemented strategies.

*Table 1. Data collection strategies for taking the ZEB-REVO measurements. Every strategy has a short description, number of repeated measurements, and an abbreviation that is used in the text.*

<i>Measurement strategy</i>	<i>Number of measurements</i>	<i>Abbreviation</i>
<i>Walking around the buildings</i>	<i>3</i>	<i>WalkR</i>
<i>Walking back and forth</i>	<i>2</i>	<i>WalkBF</i>
<i>Walking with inner loops</i>	<i>1</i>	<i>Loops</i>

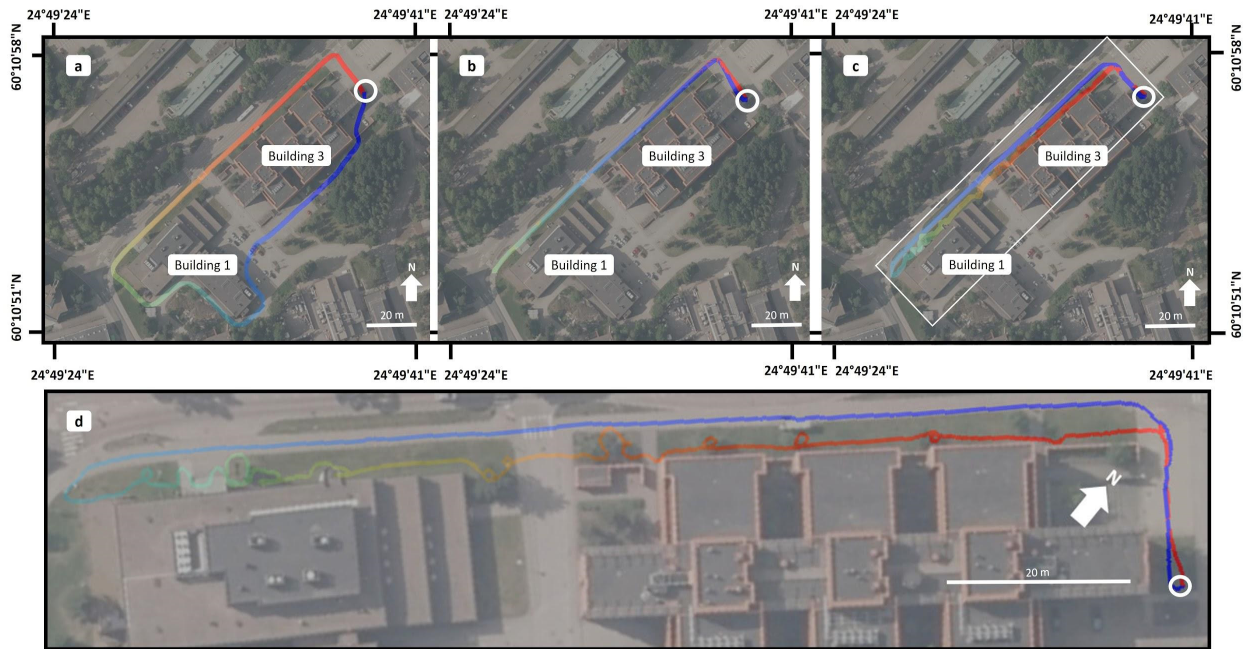


Figure 4. The ZEB-REVO measurement paths are shown by the rainbow-colored line. The line colorization is from red at the start to blue at the end. The starting and ending points of each trajectory are marked with white circle. The mapping paths are shown for strategies WalkR (a), WalkBF (b), Loops (c), and zoomed path of Loops from white rectangle (d). (Ortophotograph © Espoo City Survey Department, 2017)



Figure 5. The building facades and objects of the study area.

The ZEB-REVO measurements were registered using the GeoSLAM Hub software (version 4.1.1) with its basic settings. The output point cloud format was set to ‘LAS’ and the point cloud density was set to 100% with shaded colors. In addition to these settings, we limited the processing of the measurement paths around the buildings (1 and 3) to cover only the area of interest. Because of this, we also set the start and stop points of the scan paths at different locations. During the processing, the data was set to be registered in ‘single floor’ mode and to prioritize the planar surfaces, as these were expected to be found from the study site, and virtually in most urban environments. In addition to these settings, we calculated the colorization for the ZEB-REVO point clouds according to time of observation in the GeoSLAM Hub software. The data collection and processing elapsed times for each data set are listed in Table 2.

Table 2. Data collection of the study area and processing times of ZEB-REVO and the terrestrial laser scanner reference.

<i>Measurement strategy</i>	<i>Data collection time</i>	<i>Processing time</i>
<i>WalkR1-3</i>	<i>3,5 min</i>	<i>8 min</i>
<i>WalkBF1</i>	<i>5.5 min</i>	<i>11 min</i>
<i>WalkBF2</i>	<i>6 min</i>	<i>12 min</i>
<i>Loops</i>	<i>8.5 min</i>	<i>16 min</i>
<i>Reference</i>	<i>4 h</i>	<i>2 h</i>

## 2.4 Analysis Methods

In order to analyze the measurement strategies, we started by comparing the collected data sets with the reference point cloud in Cloud Compare. First, the registered point clouds and the reference were manually cleaned to eliminate error points. The point cloud was segmented into several subsets such as 1) building walls, 2) sidewalk and 3) the objects on the street side. After this, the point clouds were fit to the reference at first manually and then by using an iterative closest point (ICP) registration method. The parameters of ICP were 30 iterations, 50 % overlap and removed farthest points.

Following the ICP, we analyzed the root mean square error (RMSE), skewness and the mode of error, which is the most frequent difference from reference (Thomson et al. 2013, Tucci et al. 2018, Nocerino et al. 2017, and Khalloufi et al 2020). The skewness was used for analyzing the distribution of the errors. For the mode of error in case of walls and sidewalk point clouds we used the Multiscale Model to Model Cloud Comparison (M3C2) plugin (Lague et al. 2013) with Weibull fitting. We chose Weibull fitting, because of the remaining ranging noise in the data. From the M3C2 calculations, we obtained the difference between the ZEB-REVO point cloud and the reference surface model.

In addition to the aforementioned point cloud comparison metrics, we chose objects such as trees, poles, planar surfaces and building corners based on visibility in the reference point cloud and estimated their positional differences between the point clouds. The ICP registered point clouds were sliced between the heights 0.8 m - 0.95 m. From these slices, we manually measured the 2D differences to the reference point cloud in CloudCompare as in Figure 6. After the manual measurements we calculated the average differences to the reference.

Because the measurements were executed next to the busy road, we calculated the number of passed vehicles during the measurements. This was done manually from videos that were recorded during the measurements with the attached camera. Additionally, we marked the approximate locations of the passing vehicles on the orthographic image. We separated the vehicles according to type into cars and busses. We combined this data with the SLAM condition trajectory information, which was calculated in the GeoSLAM Hub software. The colors change according to SLAM conditions starting from blue (good) via yellow to red (poor), as seen in Figure 11. A diagram of the analysis process is presented in Figure 7.

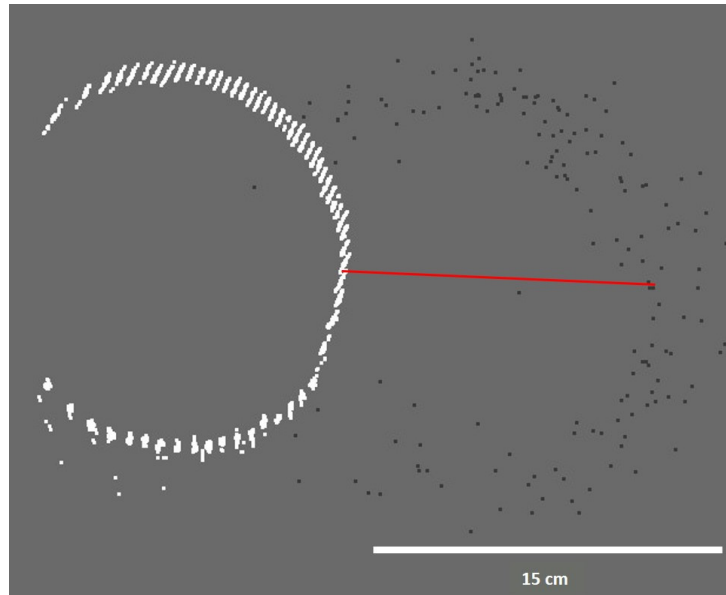


Figure 6. An illustration of 2D measurements. White point cloud is reference and the ZEB-REVO point cloud is back. The red line illustrates the distance between picked points of each point cloud.

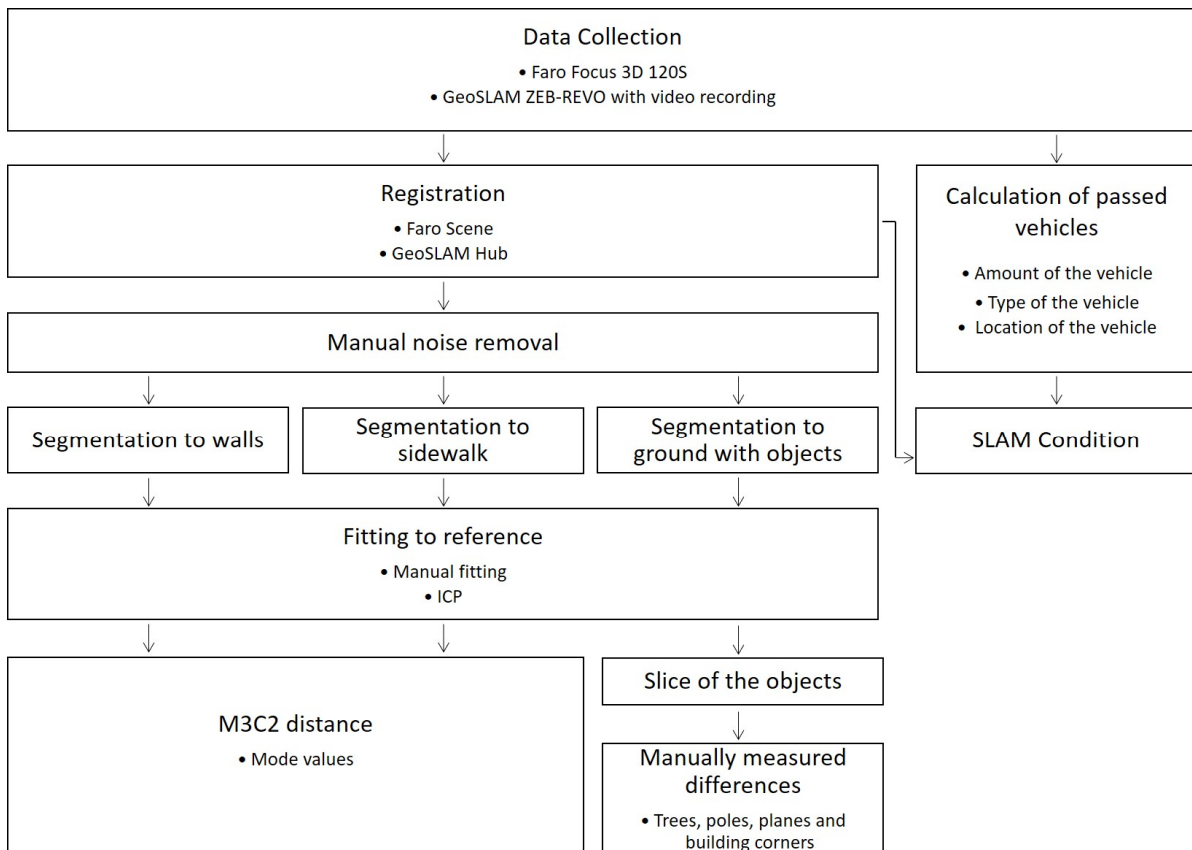


Figure 7. The diagram of the steps of the data collection and analysis.

### 3. RESULTS

The results of the ICP registration and M3C2 distance calculations are presented in Table 3, and Figure 8 and 9. The results of manually measured differences to the reference are presented in Table 3 and examples of the object types are in Figure 10. The number of passed vehicles and SLAM conditions are presented in Table 4 and Figure 11.

*Table 3. The results of the RMSE come from the ICP calculations, and the mode of error distance from the CloudCompare M3C2 plugin calculations of the different measuring methods for the wall and sidewalk point clouds. The differences to the references of the objects are calculated from the manual measurements.*

	<i>WalkBF1</i>	<i>WalkBF2</i>	<i>WalkR1</i>	<i>WalkR2</i>	<i>WalkR3</i>	<i>Loops</i>
<i>Walls</i>						
<i>RMSE walls (m)</i>	<i>0.017</i>	<i>0.017</i>	<i>0.022</i>	<i>0.017</i>	<i>0.02</i>	<i>0.02</i>
<i>Mode of error, walls (m)</i>	<i>0.32</i>	<i>0.074</i>	<i>-0.031</i>	<i>-0.022</i>	<i>-0.03</i>	<i>0.006</i>
<i>Skewness of error, walls</i>	<i>-0.81</i>	<i>-0.76</i>	<i>-0.842</i>	<i>-0.814</i>	<i>-0.733</i>	<i>-0.634</i>
<i>Sidewalk</i>						
<i>RMSE sidewalk (m)</i>	<i>0.013</i>	<i>0.017</i>	<i>0.018</i>	<i>0.02</i>	<i>0.022</i>	<i>0.012</i>
<i>Mode of error, sidewalk (m)</i>	<i>-0.007</i>	<i>-0.008</i>	<i>-0.019</i>	<i>-0.031</i>	<i>-0.011</i>	<i>-0.004</i>
<i>Skewness of error, sidewalk</i>	<i>0.219</i>	<i>0.31</i>	<i>0.187</i>	<i>0.202</i>	<i>0.797</i>	<i>0.372</i>
<i>Objects</i>						
<i>RMSE objects (m)</i>	<i>0.012</i>	<i>0.014</i>	<i>0.014</i>	<i>0.014</i>	<i>0.018</i>	<i>0.014</i>
<i>Average difference to reference (m)</i>	<i>0.136</i>	<i>0.145</i>	<i>0.105</i>	<i>0.171</i>	<i>0.12</i>	<i>0.062</i>
<i>Minimum difference to reference (m)</i>	<i>0.039</i>	<i>0.012</i>	<i>0.005</i>	<i>0.035</i>	<i>0.025</i>	<i>0.011</i>
<i>Maximum difference to reference (m)</i>	<i>0.263</i>	<i>0.254</i>	<i>0.191</i>	<i>0.319</i>	<i>0.398</i>	<i>0.119</i>
<i>Average amount of points in object slices (pcs.)</i>	<i>29</i>	<i>113</i>	<i>17</i>	<i>20</i>	<i>17</i>	<i>428</i>

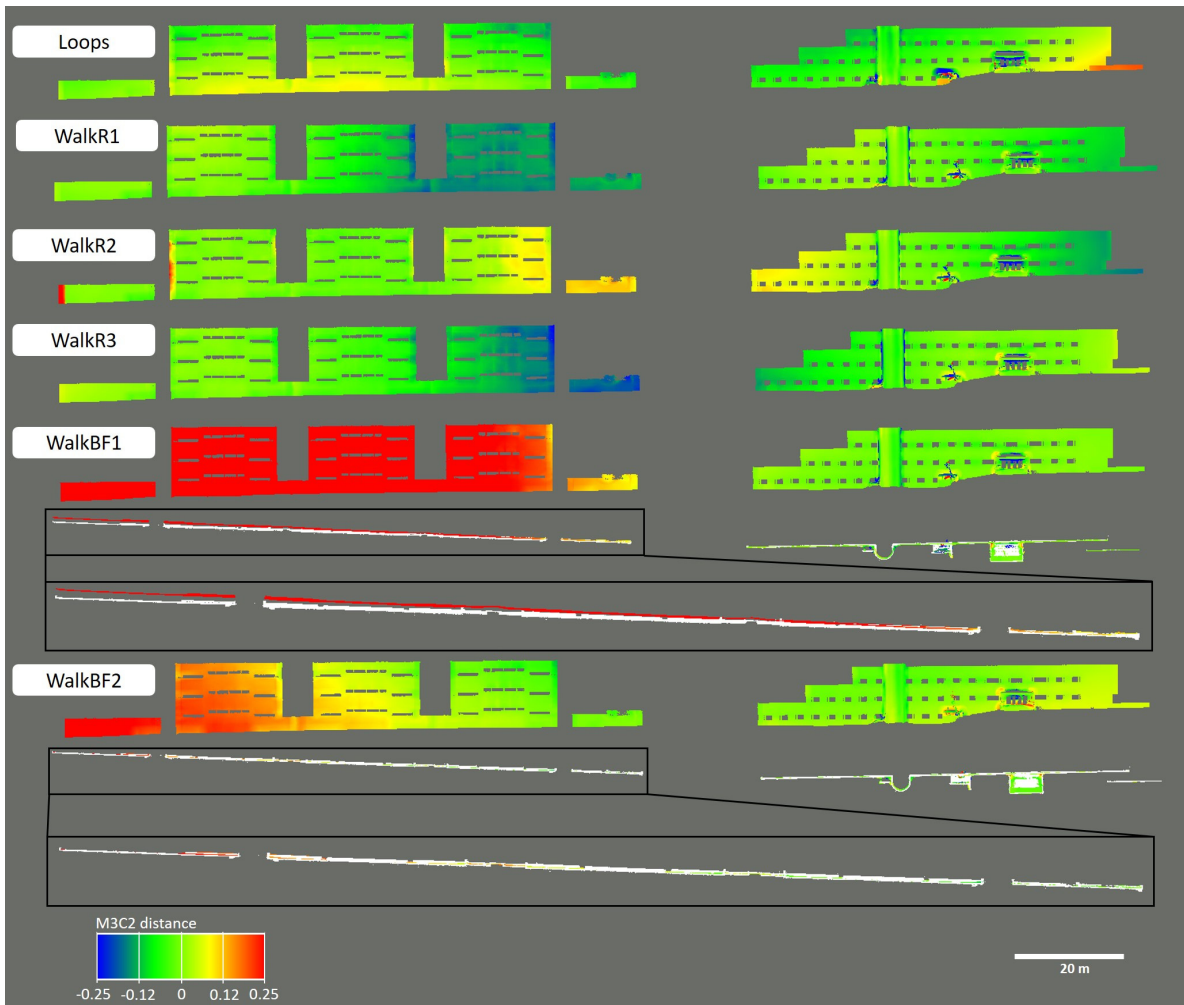


Figure 8. Visual representation of the M3C2 calculations of the walls where the distance of the ZEB-REVO measurements are projected onto the reference point cloud. There is also a top view of the WalkBF1 and WalkBF2 with a white reference point cloud and a zoom in on a section of building 3.

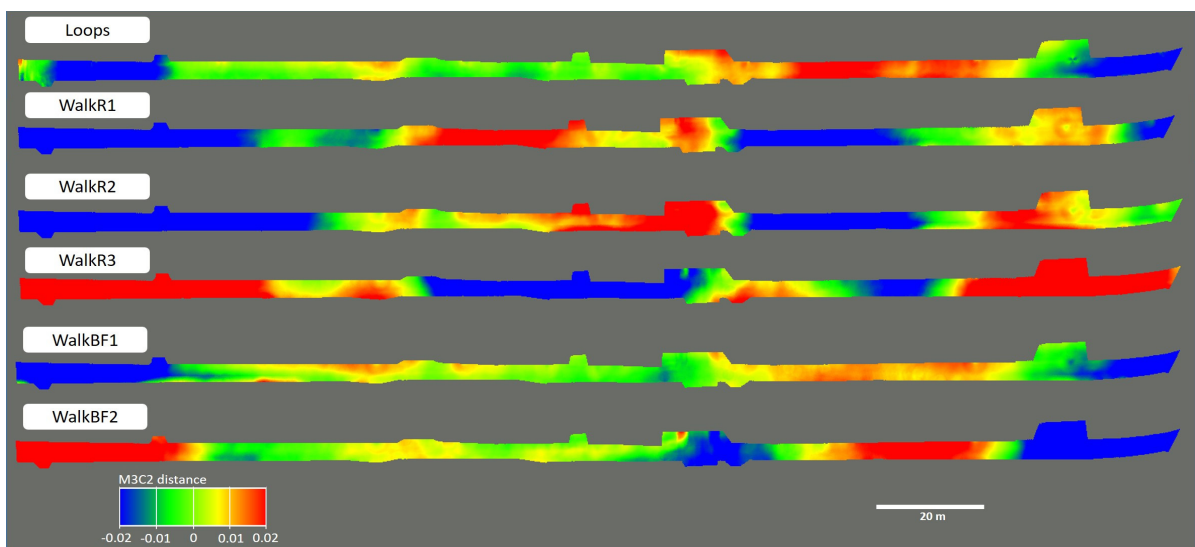


Figure 9. Visual representation of the M3C2 calculations of the sidewalk where the distance of the ZEB-REVO measurements are projected onto the reference point cloud. All distances range from  $-0.02$  to  $0.02$  m.

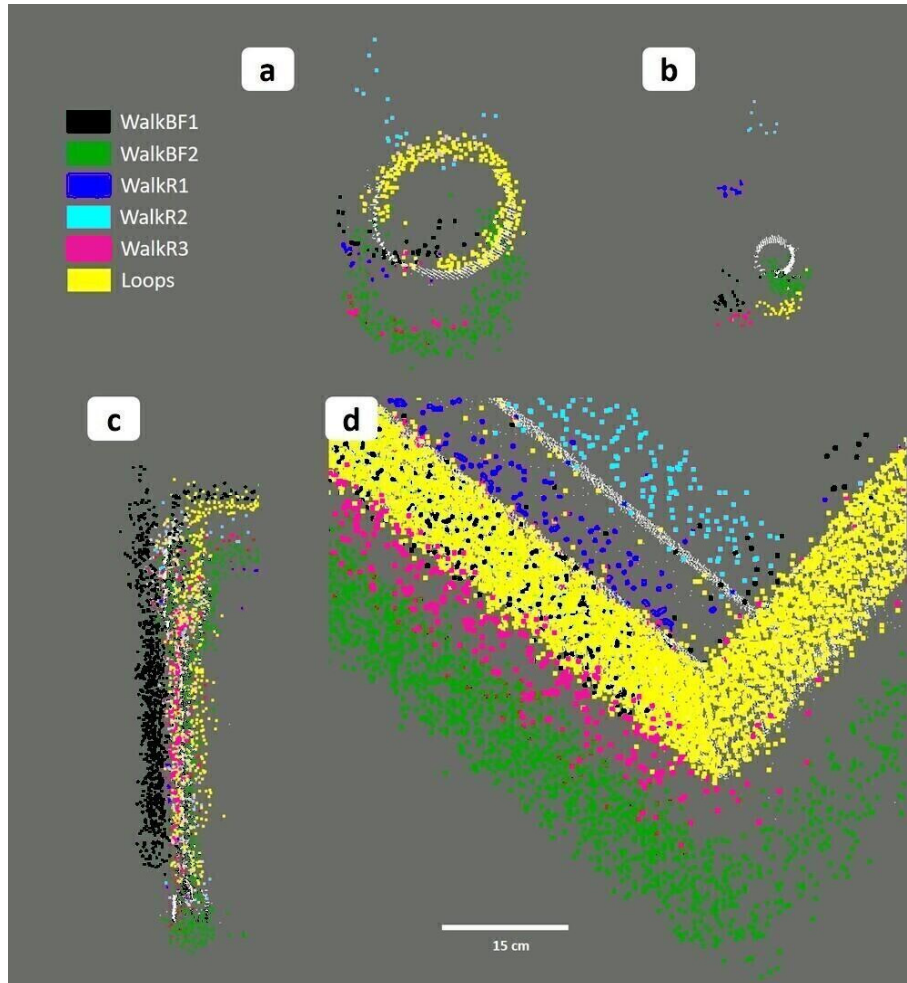


Figure 10. The objects include a) trees b) poles c) plane surfaces and d) building corners. The point cloud collected using each strategy has a unique color, and the reference point cloud is plotted in white.

Table 4. The number of passed vehicles. The vehicle results are separated based on measurement direction and the type of the vehicle.

	WalkBF1	WalkBF2	WalkR1	WalkR2	WalkR3	Loops
Amount of passed cars from start to middle (pcs)	18	5	-	-	-	14
Amount of passed cars from middle to end (pcs)	13	8	-	-	-	13
Total of passed vehicles (pcs)	31	13	13	14	11	27
Amount of passed busses (pcs)	7	3	3	4	4	6

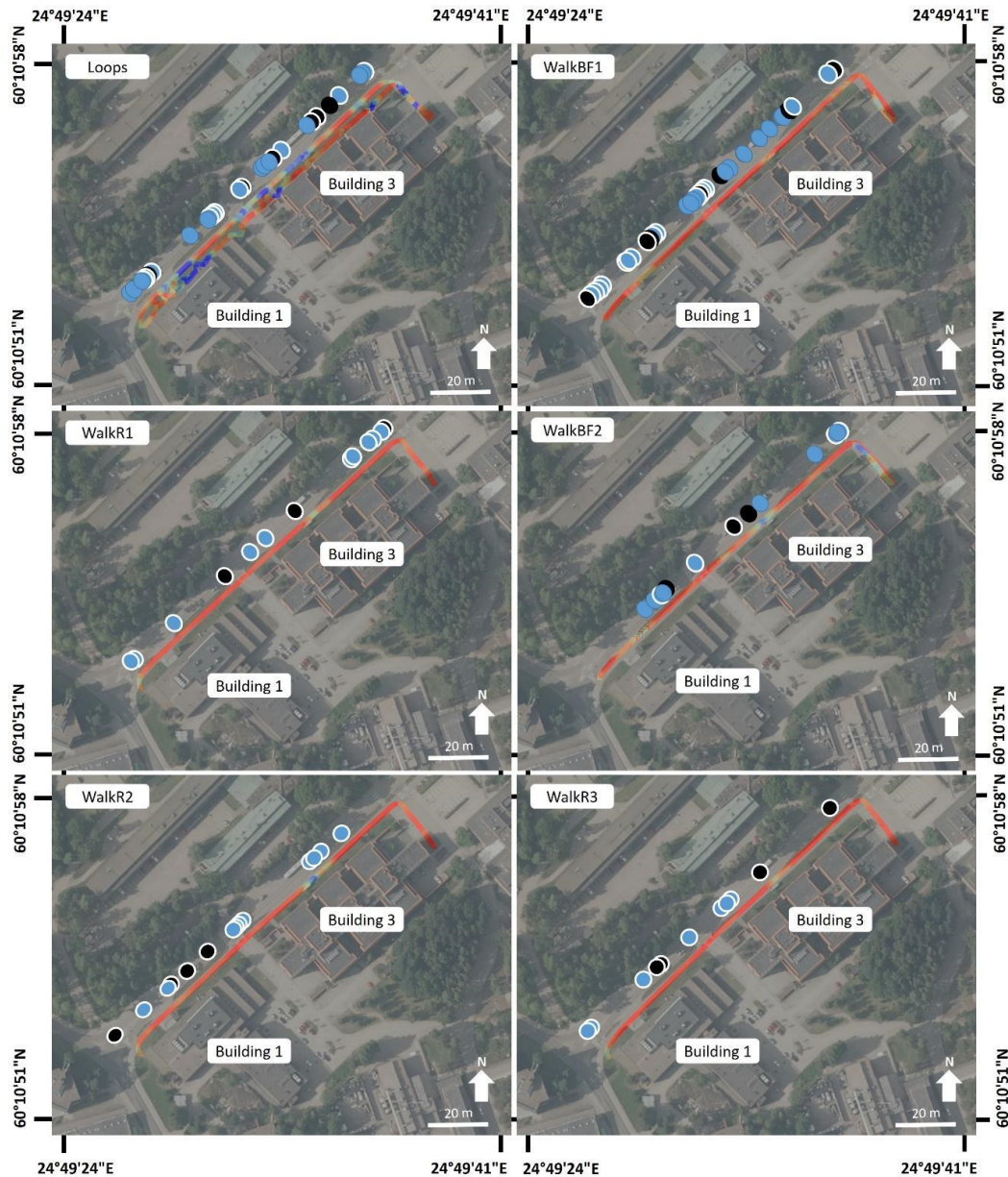


Figure 11. The SLAM conditions of the trajectories are colored from good (blue) to poor (red). The locations of the passing vehicles are marked with blue circles (cars) and with black circles (buses). The White border of the circle shows that the vehicle was passing during the first direction of the measurement. (Ortophotograph © Espoo City Survey Department, 2017)

## 4. DISCUSSION

### 4.1 Comparison of measurement strategies

Based on the results, measurement strategy clearly affects the street-level mapping. The WalkR strategy detects building walls and sidewalks with the mode of error of 1-3 cm (Table 3). However, with this strategy the average differences of the locations of street side objects were 10-17 cm from the reference. This method can map the walls and ground, but locating smaller objects such as trees and poles are more uncertain. The sidewalks do not have much noise because the error distribution is fairly symmetrical except in the WalkR3 case (skewness 0.80) However, the walls are noisy,

because the data is moderately skewed (skewness -0.73 and -0.84). The objects are detected only once in one direction, which leaves out a large amount of data regarding small objects. However, with this method we can quickly map large planar objects on the street-level. Additionally, based on the results the measurements can be repeated and the results seem to stay consistent.

Applying WalkBF strategy the sidewalk can be detected in a mode of error of 1 cm (Table 3). It has marginal noise because the skewness is 0.22-0.31, which is fairly symmetrical. For the rest of the objects the mode of errors is between 7-32 cm and the difference from the reference for the objects is 14-15 cm. On the walls, the noise is slightly less than in the case of WalkR strategy, with skewness of -0.76 and -0.81. When comparing WalkR1-3 and WalkBF1-2 results for the smaller street side objects there is not much difference. However, the cases WalkBF1-2 present a more comprehensive dataset with double or more points for the objects. Nevertheless, the duration of data collection differs 35-57 % from the WalkR and Loops strategies. These strategies give better results for the street-level object mapping than WalkBF.

The comparison of the Loops strategy (Table 1) with the others reveals that it has the smallest difference between the reference (Table 3) in every category. The mode of error in case of walls was 6 mm, which is five times smaller than with WalkR1-3, 11 times smaller than with WalkBF2 and 53 times smaller than with WalkBF1. The walls are closest to symmetrical with a skewness of -0.63. However, it is moderately skewed and lightly noisy. The mode of error in case of the sidewalk was 4 mm, which is five times smaller than with WalkR1-3 and 2 times smaller than with WalkBF1-2. The skewness of the sidewalk is fairly symmetrical (0.37). The only larger variation from reference (average 6.2 cm) is with small street side objects.

SLAM could improve city modeling, because the accuracy is the same as with MLS (Kaartinen et al. 2012, and Barber et al. 2008) and it can reach GNSS free areas. Street-level mapping by the SLAM-based laser scanners could be used for monitoring land use, façade deterioration and vegetation, as a base of new plans and analyzing for example safety and pavement condition and street infrastructure. However, there are some supposedly problematic areas for the SLAM algorithm in urban environments such as large parking lots and other such areas with limited geometric features, and narrow, possibly featureless, and repetitive lanes. In particular, open areas where the ranging capability of the scanner does not reach vertical planes, or point density is not enough for capturing other features, present a challenge. These environments do not have enough noticeable features for the SLAM algorithms. In addition, the missing or only partially colored data from the SLAM-based laser scanners are reducing the feasibility of the devices at the moment (Sammartano & Spanò 2018, and Sammartano et al. 2019). However, a solution for the point cloud colorization will help them to complement, or even replace terrestrial laser scanners in the street-level mapping of urban environments. In addition, the use of longer trajectories would require further studies because of possible drift errors and in order to create methods for correcting these errors.

## **4.2 Influence of passing vehicles on SLAM**

The traffic did not have a significant influence on the WalkR strategies. The SLAM condition was poor in the respective locations (Figure 11) even though the passing vehicles were not present in these locations. However, at the end of the WalkR2 there were four busses detected passing by and the SLAM condition was better in that location than in the WalkR1 and WalkR3. Even though the SLAM condition was better, the resulting point cloud has ca. 1 cm larger difference between the mode of error values than those of WalkR1 and WalkR3. Based on this the busses that were passing by in a row had a small negative influence on the SLAM even though the SLAM condition

was seemingly better. We assume this is caused by the SLAM algorithm finding planar features from the passing busses, thus resulting in a "better" indicated SLAM condition, but leading to incorrect results, as these features are not in reality stationary. However, it is the only place where the repeated methods differ in SLAM condition values from each other.

On comparing the traffic and the strategies, Loops and WalkBF1 had almost the same number of passing vehicles observed during the measurements. However, the SLAM conditions were more good for the Loops (Table 4). This shows that the traffic does not influence significantly when the sensor can observe stable landmarks while vehicles are passing by. These are locations where the SLAM condition was estimated good, and the data collection had been done with the loops (Figure 11). It improves the performance and reliability of the SLAM. Additionally, the mode of errors and the difference from the reference values (Table 3) for WalkBF1 were weaker than those for the Loops strategy.

The amount of traffic has an influence on the resulting point cloud such as is the case with the repeated WalkBF1 and WalkBF2 measurements. The WalkBF1 method has the largest variation of distances from the reference (Figure 8) and the largest mode of error (32 cm) (Table 3). The reason for these large values can be traced to an erroneous change in the angle between the buildings. In practice, building 3 appears slightly rotated (Figure 8) in the scan. The change on the angle can be due to the combination of traffic and the gap between the buildings (Figure 2) to create drift in the data. There were 7 vehicles passing when the measurement path was executed in the gap. These could have given some fake planar surfaces for the SLAM calculations. For these reasons we repeated the measurement with less traffic conditions.

In the visual representation of the walls, the WalkBF2 shows that it fits the reference better than WalkBF1 (Figure 8). However, there is still a small part of building 3 that differs from the reference. The reason for the difference is that during the first time the erroneous area was observed the SLAM had problems because of vehicles passing around the corner (Figure 8 and 11). For the second observation it was slightly improved, but the SLAM solution had again problems for a moment because of passing vehicles. Despite the large difference between the mode of errors for the walls (WalkBF1 32 cm and WalkBF2 7.4 cm), the mode of error for the sidewalk was the same for both of the strategies (ca. 1 cm).

Based on these results traffic with speed of ca. 40 km/h has an impact on the SLAM. Comparing the SLAM conditions of the WalkBF1 with 31 passed vehicles and WalkBF2 with 13 passed vehicles. It seems that every vehicle makes SLAM conditions poor for a moment and the longest effect was noted in the return direction in the gap when the bus passed just before the gap between the buildings (Figure 11). However, next to the bus stop the SLAM condition is good despite the passing vehicles in every strategy. It offers many planar features for the SLAM to locate itself. In conclusion, it is recommended to avoid traffic at open and featureless areas such as gaps between buildings.

Accurately quantifying the influence of traffic on SLAM performance in urban scenes would require further experiments. The influence of traffic on the performance of the SLAM can be investigated with comparison of data collected in zero traffic conditions to that in presence of traffic. Also, the motion (speed, direction, frequency, vehicle size and size distribution, distance to the scanner) of the traffic should be determined so that the opportunities and limitations of SLAM technology in city modeling could be better identified. Thus, it could be determined whether certain traffic velocities have a lesser influence on the SLAM performance.

## 5. CONCLUSIONS

In this study, the aim was to evaluate the impact of different measurement strategies on performance of SLAM laser scanning for mapping street-level urban environments looking at the potential influence of different measurement strategies. From the results of the case study, it can be concluded that the measurement strategy affects the performance of street-level mapping. The best results were obtained with the Loops strategy, forming the maximal number of closed loops in the walking path by e.g. circling individual trees. However, big street side objects such as building walls and the ground can be measured faster with the WalkR strategy. The WalkBF strategy does not improve the performance enough in comparison to WalkR1-3 and Loops to be truly feasible for street-level mapping. However, the study was executed in a challenging environment for the ZEB-REVO laser scanner. The differences between the strategies may be smaller in an environment with many features.

The results indicate that traffic should be considered in planning and during the measurement. The effect of traffic was smallest with Loops because of many stable landmarks present in the scan. In the WalkR strategy the influence of traffic was more pronounced, but still rather small with a mode of errors under 3 cm in repeated measurements. The influence was largest with the WalkBF strategy. In terms of attained accuracy, the Loops strategy is therefore the best for street-level mapping, but it can be replaced with WalkR strategy if faster data collection is needed. The WalkBF strategy does not give enough benefits to be used as a measurement strategy for street-level mapping.

## ACKNOWLEDGEMENTS

Funding: This research was funded by the Centre of Excellence in Laser Scanning Research (CoE-LaSR) (No. 272195, 307362), “Competence-Based Growth Through Integrated Disruptive Technologies of 3D Digitalization, Robotics, Geospatial Information and Image Processing/Computing–Point Cloud Ecosystem”, pointcloud.fi (No. 293389), ”Multi-spectral personal laser scanning for automated environment characterization” (No. 300066), “Quality4Roads” (No. 323783), “Profi5 Autonomous systems” (No. 326246), The City of Helsinki Innovation Fund project “Helsinki Smart Digital Twin 2025” and Aalto University School of Engineering Tenure track (Digital Photogrammetry) funding.

Acknowledgments: The authors would like to thank Toni Rantanen, Sami-Petteri Karvonen, Helmi Takala and Iris Nurminen for assisting in the terrestrial laser scanning acquisitions.

## REFERENCES

Adán, A., Quintana, B., and Prieto, S. A., 2019. Autonomous Mobile Scanning Systems for the Digitization of Buildings: A Review. *Remote Sensing*, Vol. 11, pp. 306-327. doi.org/10.3390/rs11030306

Barber, D., Mills, J., and Smith-Voysey, S., 2008. Geometric validation of a ground-based mobile laser scanning system. *ISPRS Journal of Photogrammetry and Remote Sensing*. Vol. 63, No. 1, pp. 128-141. doi.org/10.1016/j.isprsjprs.2007.07.005

Bosse, M., Zlot, R., and Flick, P., 2012. Zebedee: Design of a Spring-Mounted 3-D Range Sensor with Application to Mobile Mapping. *IEEE Transactions on robotics*, Vol. 5, pp. 1104-1119. doi: 10.1109/TRO.2012.2200990

Cabo, C., Del Pozo, S., Rodríguez-Gonzálvez, P., Ordóñez, C., and González-Aguilera, D., 2018. Comparing Terrestrial Laser Scanning (TLS) and Wearable Laser Scanning (WLS) for Individual Tree Modeling at Plot Level. *Remote sensing*, Vol. 10, pp. 540-556. doi: 10.3390/rs10040540

Cadge, S., 2016. Welcome to the ZEB REVolution. *Geomedica*, Vol. 3, pp. 22-25.

Chiabrando, F., Della Coletta, C., Sammartano, G., Spanò, A., and Spreafico, A., 2018. "Torino 1911" project: A Contribution of a SLAM-based Survey to Extensive 3D Heritage Modelling. *The International Archives of the Photogrammetry, Remote Sensing and Spatial Information Sciences*, XLII-2, Riva Del Garda, Italy, 4-7 June 2018, pp. 225-234.

City of Helsinki, 2019. Available online:

<https://www.hel.fi/helsinki/en/administration/information/general/3d/how-were-the-3D-models-made/> (accessed on 7 August 2019).

Dewez, T. J. B., Yart, S., Thuon, Y., Pannet, P., and Plat, E., 2017. Towards Cavity-Collapse Hazard Maps With ZEB-REVO Handheld Laser Scanner Point Clouds. *The Photogrammetric Record*, Vol. 32, pp. 354-376. doi: 10.1111/phor.12223

Dewez, T., Plat, E., Degas, M., Richard, T., Pannet, P., Thuon, Y., Meira, B., Watelet, J-M., Cauvin, L., Lucas, J., and Dian, G., 2016. Handheld Mobile Laser Scanners Zeb-1 and Zeb-Revo to map an underground quarry and its above-ground surroundings. *2nd Virtual Geosciences Conference: VGC 2016*, Bergen, Norway, September 2016, 2 pages.

ETHZurich., 2019. Available online: <https://ethz.ch/en/news-and-events/eth-news/news/2017/05/city-model-created-from-images-alone.html> (accessed on 7 August 2019).

Eyre, M., Wetherelt, A., and Coggan, J., 2016. Evaluation of automated underground mapping solutions for mining and civil engineering applications. *J. Applied Remote Sensing*, Vol. 4, pp. 046011-1-046011-18. doi: 10.1117/1.JRS.10.046011

Farella, E., Menna, F., Nocerino, E., Morabito, D., Remondino, F., and Campi, M., 2016. Knowledge and valorization of historical sites through 3D documentation and modeling. *The International Archives of the Photogrammetry, Remote Sensing and Spatial Information Sciences*, Prague, Czech Republic, 12-19 July 2016. doi: 10.5194/isprsarchives-XLI-B5-255-2016

Frangez, V., Kramis, B., Hübscher, F., and Baumann, A., 2018. Comparison of Three Innovative Technologies for 3D-Acquisition, Modelling, and Visualization of an Underground Mine. *FIG Congress 2018*, Istanbul, Turkey, 6-11 May 2018.

GeoSLAM, 2017. ZEB-REVO User guide, <https://www.sccsurvey.co.uk/pdfs/HDS/GeoSLAM-ZEB-REVO-User-Guide.pdf> (accessed on 18 November 2020).

GIM, 2019. Available online: <https://www.gim-international.com/content/article/3d-city-modelling-of-istanbul> (accessed on 7 August 2019).

- Haala, N., Peter, M., Kremer, J., and Hunter, G., 2008. Mobile LIDAR Mapping for 3D Point Cloud Collection in Urban Areas - A Performance Test. *The International Archives of the Photogrammetry, Remote Sensing and Spatial Information Sciences*, 37, Beijing, China, 3-11 July 2008, pp. 1119-1124.
- Holland, D. A., Pook, C. Capstick, D., and Hemmings, A., 2016. The Topographic data deluge - collecting and maintaining data in a 21st century mapping agency. *The International Archives of the Photogrammetry, Remote Sensing and Spatial Information Sciences*, Volume XLI-B4, Prague, Czech Republic, 12-19 July, 2016, pp. 727-731. doi: 10.5194/isprsarchives-XLI-B4-727-2016
- Kaartinen, H., Hyypä, J., Kukko, A., Jaakkola, A., and Hyypä, H., 2012. Benchmarking the Performance of Mobile Laser Scanning Systems Using a Permanent Test Field. *Remote sensors*. Vol. 12, No. 9, pp. 12814-12835. doi: 10.3390/s120912814
- Khalloufi, H., Azough, A., Ennahahi, N., and Zahra Kaghat, F., 2020. Low-cost terrestrial photogrammetry for 3d modeling of historic sites: a case study of the marinids' royal necropolis city of fez, morocco. *Mediterranean Archaeology and Archaeometry*. Vol. 20, No. 3, pp. 257-272. doi: 10.5281/zenodo.3930412
- Kukko, A., Kaijaluoto, R., Kaartinen, H., Lehtola, V. V., Jaakkola, A., and Hyypä, J., 2017. Graph SLAM correction for single scanner MLS forest data under boreal forest canopy. *ISPRS Journal of Photogrammetry and Remote Sensing*, Vol. 132, pp. 199-209. doi: 10.1016/j.isprsjprs.2017.09.006
- Lague, D., Brodu, N., and Leroux, J., 2013. Accurate 3D comparison of complex topography with terrestrial laser scanner: application to the Rangitikei canyon (N-Z). *ISPRS Journal of Photogrammetry and Remote Sensing*, Vol. 82, pp. 10-26. doi: 10.1016/j.isprsjprs.2013.04.009
- Lee, J. and Yang, B., 2018. Developing an optimized texture mapping for photorealistic 3D buildings. *Transaction in GIS*, Vol. 23, pp. 1-21. doi: 10.1111/tgis.12494
- Lehtola, V. V., Kaartinen, H., Nüchter, A., Kaijaluoto, R., Kukko, A., Litkey, P., Honkavaara, E., Rosnell, T., Vaaja, M. T., Virtanen, J-P., Kurkela, M., El Issaoui, A., Zhu, L., Jaakkola, A., and Hyypä, J., 2017. Comparison of the Selected State-Of-The-Art 3D Indoor Scanning and Point Cloud Generation Methods. *Remote sensing*, Vol. 9, pp. 796-822. doi: 10.3390/rs9080796
- Ma, L., Li, Y., Li, J., Wang, C., Wang, R., and Chapman, M. A., 2018. Mobile Laser Scanner Point-clouds for Road Object Detection and Extraction: Review. *Remote Sensing*, Vol. 10, pp. 1531-1564. doi: 10.3390/rs10101531
- Maboudi, M., Bánhidi, D., and Gerke, M., 2017. Evaluation of indoor mobile mapping systems. *GFaI Workshop 3D North East 2017 (20th Application-oriented Workshop on Measuring, Modeling, Processing and Analysis of 3D-Data)*, Berlin, Germany, December 2017, pp. 125-134.
- Manan Samad, A., Badrul Hafiz, M., Omar, C., Sahrma, N., Johar, J., Ahmat Ruslan, F., and Adna R., 2016. Implementation of Zebedee 3D Laser Scanner Sensor for Preparation of Strata Title Plan. *IEEE 7th Control and System Graduate Research Colloquium*, Shah Alam, Malaysia, 8 August 2016. doi: 10.1109/ICSGRC.2016.7813329

- Micoli, L., Gonizzi Barsanti, S., Malik, U., and Guidi, G., 2018. 3D data integration for the digital reconstruction of cultural heritage monuments. IOP Conf. Series: Materials Science and Engineering, Florence, Italy, 16-18 May 2018. doi: 10.1088/1757-899X/364/1/012043
- Nebiker, S., Bleisch, S., and Christen, M., 2010. Rich point cloud in virtual globes - A new paradigm in city modeling? Computers, Environment and Urban Systems, Vol. 34, pp. 508-517. doi: 10.1016/j.compenvurbsys.2010.05.002
- Nocerino, E., Menna, F., Remondino, F., Toschi, I., and Rodríguez-González, P., 2017. Investigation of indoor and outdoor performance of two portable mobile mapping systems. SPIE Optical Metrology, Munich, Germany, 26 June 2017. doi: 10.1117/12.2270761
- Rotterdam. 2019. Available online: <https://www.rotterdam.nl/werken-leren/3d/> (accessed on 7 August 2019).
- Sammartano, G., Spanò, A., and Teppati Losè, L., 2019. A Fusion-based Workflow For Turning Slam Point Clouds And Fisheye Data Into Texture-enhanced 3D Models. The International Archives of the Photogrammetry, Remote Sensing and Spatial Information Sciences, XLII-2/W17, Strasbourg, France, 2-3 December, pp. 295-302. doi: 10.5194/isprs-archives-XLII-2-W17-295-2019
- Sammartano, G. and Spanò, A., 2018. Point clouds by SLAM-based mobile mapping systems: accuracy and geometric content validation in multisensor survey and stand-alone acquisition. Applied Geomatics, pp. 1-23. doi: 10.1007/s12518-018-0221-7
- Sepasgozar, S .M. E., Lim, S.M., Shirowzhan, S., and Kim Y. M., 2014. Implementation of As-Built Information Modelling Using Mobile and Terrestrial Lidar Systems. The 31st International Symposium on Automation and Robotics in Construction and Mining, Sydney, Australia, 9-11 July 2014. doi: 10.13140/2.1.1226.3689
- Sirmacek, B., Shen, Y., Lindenbergh, R., Zlatanova, S., and Diakite, A., 2016. Comparison of ZEB1 and Leica C10 indoor laser scanning point clouds. The International Archives of the Photogrammetry, Remote Sensing and Spatial Information Sciences, III-1, Prague, Czech Republic, 12-19 July, 2016, pp. 143-149. doi: 10.5194/isprsannals-III-1-143-2016
- Staats, B. R., Diakité, A. A., Voûte, R. L., and Zlatanova, S., 2017. Automatic generation of indoor navigable space using a point cloud and its scanner trajectory. ISPRS Annals of the Photogrammetry, Remote Sensing and Spatial Information Sciences, Vol. IV-2, No. W4, pp. 393-400. doi: 10.5194/isprs-annals-IV-2-W4-393-201
- So, A. C. T., Pau, L. L. Y., Jonas, D., and Weigler, B., 2015. A Pilot study on the use of handheld laser scanner for landform mapping and slope investigation in Hong Kong. 36th Asian Conference on Remote Sensing 2015, Quezon City, Metro Manila Philippines, 19-23 October 2015, Lagmay, A., M., Asian Association on Remote Sensing, Tokyo, Japan, 2015, 11 pages. ISBN: 978-1-5108-1721-0
- Thomson, C., Apostolopoulos, G., Backes, D., and Boehm, J., 2013. Mobile laser scanning for indoor modelling. ISPRS Workshop Laser Scanning 2013, ISPRS Annals of the Photogrammetry, Remote Sensing and Spatial Information Sciences, II-5/W2, Antalya, Turkey, 11-13 November 2013, pp. 289-293. doi: 10.5194/isprsannals-II-5-W2-289-2013

Tucci, G., Visintini, D., Bonora, V., and Parisi, E. I., 2018. Examination of Indoor Mobile Mapping Systems in a Diversified Internal/External Test Field, *Applied Sciences*, Vol. 3, pp. 401-431. doi: 10.3390/app8030401

Valencia, J., Muñoz-Nieto, A., and Rodriguez-Gonzalvez, P., 2015. Virtual modeling for cities of the future. State-of-the art and future challenges. *The International Archives of the Photogrammetry, Remote Sensing and Spatial Information Sciences*, XL-5/W4, Avila, Spain, 25-27 February, 2015, pp. 179-185. doi: 10.5194/isprsarchives-XL-5-W4-179-2015

Vanneschi, C., Eyre, M., Francioni, M, and Coggan, J., 2017. The Use of Remote Sensing Techniques for Monitoring and Characterization of Slope Instability. *Procedia Engineering*, Vol. 191, pp. 150-157. doi: 10.1016/j.proeng.2017.05.166

Virtanen, J.P., Kukko, A., Kaartinen, H., Jaakkola, A., Turppa, T., Hyypä, H., and Hyypä, J., 2017. Nationwide Point Cloud—The Future Topographic Core Data. *ISPRS International Journal of Geo-Information*, Vol. 6, No. 8, 243, 18 pages.

Zhu, L., Hyypä, J., Kukko, A., Kaatinen, H., and Chen, R., 2011. Photorealistic Building Reconstruction from Mobile Laser Scanning Data. *Remote Sensing*, Vol. 3, pp. 1406-1426. doi.org/10.3390/rs3071406

Zlot, R. and Bosse, M., 2014. Three-dimensional mobile mapping of caves. *Journal of Cave and Karst Studies*, Vol. 76, pp. 191-206. doi: 10.4311/2012EX0287

Zlot, R., Bosse, M., Greenop, K., Jarzab, Z., and Juckes, E., 2014. Efficiently capturing large, complex cultural heritage sites with a handheld mobile 3D laser mapping system. *Journal of Cultural Heritage*, pp. 670-678. doi.org/10.1016/j.culher.2013.11.009